RESEARCH/REVIEW ARTICLE

Distribution of total alkalinity and pH in the Ross Sea (Antarctica) waters during austral summer 2008

Paola Rivaro,[1] Roberta Messa,[1] Carmela Ianni,[1] Emanuele Magi[1] & Giorgio Budillon[2]

[1] Department of Chemistry and Industrial Chemistry, University of Genoa, via Dodecaneso 31, IT-16146 Genova, Italy
[2] Department of Environmental Sciences, Centro Direzionale, Parthenope University, Isola C4 IT-80143 Napoli, Italy

Keywords
Total alkalinity; pH; saturation state; Terra Nova Bay polynya; Ross Sea.

Correspondence
Paola Rivaro, Department of Chemistry and Industrial Chemistry, University of Genoa, via Dodecaneso 31, IT-16146 Genova Italy.
E-mail: rivaro@chimica.unige.it

Abstract

Measurements of total alkalinity (A_T) and pH were made in the Ross Sea in January–February 2008 in order to characterize the carbonate system in the Ross Sea and to evaluate the variability associated with different water masses. The main water masses of the Ross Sea, Antarctic Surface Water, High Salinity Shelf Water (HSSW), Deep Ice Shelf Water, Circumpolar Deep Water (CDW) and Antarctic Bottom Water, were identified on the basis of the physical and chemical data. In particular, the A_T ranged between 2275 and 2374 μmol kg^{-1} with the lowest values in the surface waters (2275–2346 μmol kg^{-1}), where the influence of the sea-ice melting and of the variability of the physical properties was significant. In the deep layers of the water column, the A_T maxima were measured in correspondence to the preferential pathways of the spreading HSSW. The pH had variable values in the surface layer (7.890–8.033) with the highest values in Terra Nova Bay and Ross Sea polynyas. A low pH (7.969 ± 0.025) traced the intrusion of the CDW in the Ross Sea shelf area. All samples revealed waters that were oversaturated with respect to both calcite and aragonite, but near corrosive levels of aragonite saturation state (Ω ca. 1.1–1.2) were associated with the entrainment of CDW over the slope. Aragonite undersaturation is of particular concern for the zooplankton species comprising to calcifying organisms such as pteropods. The partial pressure of CO_2 at the sea surface was undersaturated with respect to the atmospheric value, particularly in Terra Nova Bay and the Ross Sea polynyas, but a large variability in the sea–air CO_2 fluxes was observed associated with different responses in the strength of the biological and physical processes.

The Ross Sea is an important site of deep water production (Orsi et al. 1999; Gordon, Padman et al. 2009) and one of the most biologically productive regions in the Southern Ocean (Garrison et al. 2003; Smith et al. 2003; Arrigo & Van Dijken 2004). For these reasons, the Ross Sea plays a role in the global carbon budget behaving as an atmospheric carbon dioxide (CO_2) sink. The magnitude of this sink depends on different environmental conditions and physical and biological processes. Physical processes such as the formation of Antarctic Bottom Water (AABW), which is an essential component of the global thermohaline circulation, the upwelling of the Circumpolar Deep Water (CDW) near the margin of the Ross Sea continental shelves and the pack-ice coverage can largely influence the sea–air exchange of CO_2.

The export of new deep and bottom waters produced over the continental margins of the Ross Sea, by the mixing of shelf waters (SWs) and the CDW, contributes significantly to the total ventilation of the deep Southern Ocean (Orsi & Wiederwohl 2009); it may play an important role in the sequestration of anthropogenic CO_2 transferring dissolved CO_2 into the deep ocean (Caldeira & Duffy 2000; Sabine et al. 2004; Sandrini et al. 2007). The oceanography of the Ross Sea is largely affected by the presence of polynyas (areas where the sea surface is kept free from sea ice even during the winter). In these

Citation: *Polar Research* 2014, *33*, 20403, http://dx.doi.org/10.3402/polar.v33.20403

areas, the surface seawater shows temperatures near the freezing point and is directly exposed to a large negative (sea–air) heat flux. These conditions yield fast formation of new sea ice (polynyas are often referred to as "sea-ice factories") and the rejection of brine. Brine-enriched water descends, because it is dense, allowing the injection of dissolved oxygen into the deeper layers, since it has originated from surface waters. The Terra Nova Bay polynya (TNBp) is a coastal latent heat polynya located in the western Ross Sea (Fig. 1); it is considered as the main source of High Salinity Shelf Water (HSSW), which is the densest SW of the Ross Sea, and—in turn—a fundamental component of the AABW in this region (Jacobs et al. 1985; Parish & Bromwich 1989; Bromwich et al. 1990; Budillon & Spezie 2000; Fusco et al. 2009).

The seasonal ice coverage strongly impacts the cycling of chemical species and biological processes. Significant sea-ice coverage restricts CO_2 sea–air exchange during winter in the Ross Sea and thus limits the equilibration of the Antarctic Surface Water (AASW) with the overlying atmosphere. As a result of the heterotrophic activities, the AASW is supersaturated with CO_2 and undersaturated in dissolved oxygen (O_2) (Sweeney 2003). Melting of pack-ice and warming of AASW are responsible for water column stratification, which favours the phytoplankton bloom in summer. Phytoplankton photosynthetic activities cause a reduction in the sea-surface partial pressure of CO_2 (pCO_2) and an increase of O_2. Differences in the strength of the water column stratification, in the upper mixed layer (UML) and in the algal population can account for significant differences of the pCO_2 drawdown. In particular, the CO_2 drawdown measured for diatoms is much lower than that measured for *Phaeocystis antarctica* (Arrigo et al. 1999; Feng et al. 2010). The sea-ice extension and disappearance, and consequently the sea–air exchange of CO_2 can also be impacted by large-scale climate signals (e.g., El Niño Southern Oscillation, Southern Annular Mode), as well as by large icebergs calving off the face of the Ross Ice Shelf (Arrigo & Van Dijke 2004; Massolo et al. 2009). Recently, fine-scale variability in pCO_2, in the Ross Sea polynya (RSp), located in the south-western Ross Sea at about 75.51°S, 179.21°E, has been documented,

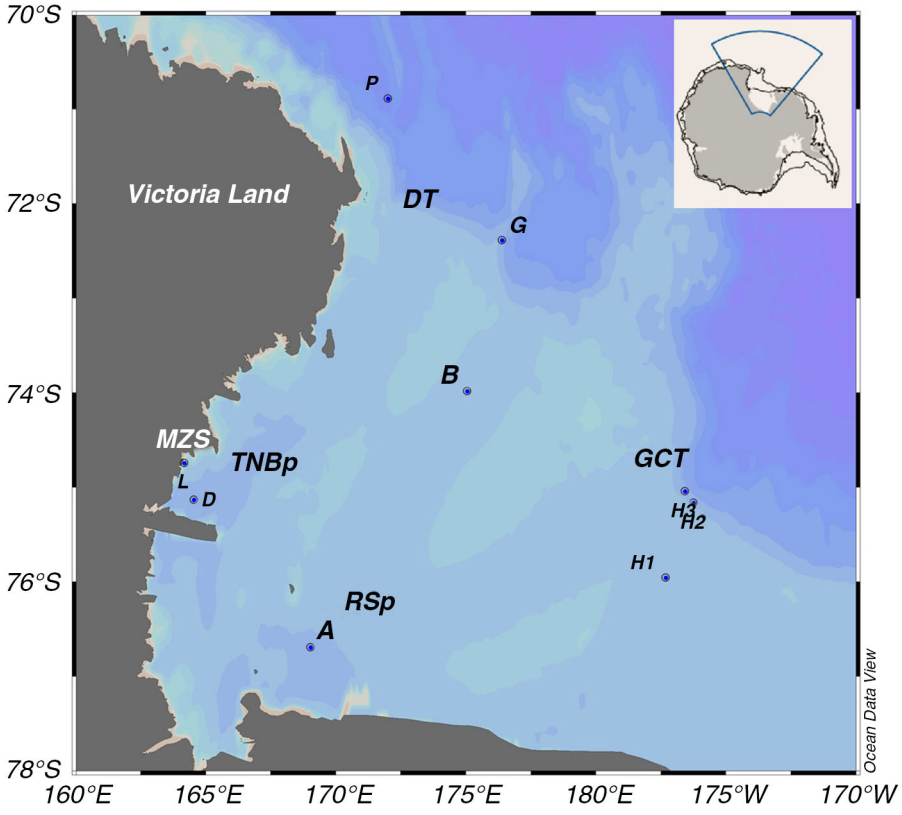

Fig. 1 Distribution of the conductivity–temperature–depth casts sampled for the carbonate system variables during Italian National Antarctic Research Program austral summer cruise 2008. The insert shows the Ross Sea inside the Southern Ocean. The areas of the Ross Sea investigated in this study are labelled: Terra Nova Bay polynya (TNBp), Ross Sea polynya (RSp), Drygalski Trough (DT), Glomar Challenger Trough (GCT). The Italian Research Station Mario Zucchelli (MZS) is shown.

Citation: *Polar Research* 2014, *33*, 20403, http://dx.doi.org/10.3402/polar.v33.20403

exhibiting significant differences between the early spring and summer. This variability was also found to be coupled to the heterogeneity in underlying physical and biological variables (e.g., sea-ice cover and chlorophyll-a) (Tortell et al. 2011).

In 2008, we were able to obtain measurements of the Ross Sea CO_2 system (pH and total alkalinity [A_T]) for the sea surface and water column during the summer season within the framework of the Italian National Antarctic Research Program (PNRA) oceanographic survey. This paper aims at characterizing the carbonate system in the Ross Sea and at evaluating the variability associated with different water masses. Moreover, it extends previous analyses carried out by PNRA by presenting new data that aids in understanding the CO_2 system distribution parameters. We will focus on the influence of the sea ice and of the physical variables on the inorganic carbon parameters distribution in the AASW, on the CO_2 air–sea fluxes and on the role of the main water masses in the distribution of inorganic carbon in the intermediate and deep layers, with particular regard for the intruding CDW in its contribution to the acidification of the Ross Sea.

Methods

Sampling

The sampling took place from 25 January to 4 February 2008, as part of the PNRA oceanographic survey of the Ross Sea. A total of 60 seawater samples were collected for measurements of pH and A_T. Stations A, H1, L, D and B are located on the continental shelf, stations H2, H3 and G over the slope, and station P offshore (Fig. 1). Information on the stations sampled is in Table 1.

Conductivity–temperature–depth (CTD) casts were performed using an SBE 911plus probe with double temperature, conductivity and oxygen sensors coupled to a SBE 32 Carousel Water Sampler (Sea-Bird Electronics, Bellevue, WA). The CTD was flushed at a constant rate, always below 1m s^{-1}.

Table 1 Dates, coordinates and depths of the stations sampled during the austral summer 2008 in the Ross Sea.

Station	Sampling date	Latitude	Longitude	Bottom depth (m)
A	30 Jan 2008	76°41.821′ S	169°02.143′ E	813
H1	28 Jan 2008	75°57.559′ S	177°18.891′ W	621
H2	29 Jan 2008	75°09.889′ S	176°14.220′ W	787
H3	29 Jan 2008	75°02.618′ S	176°34.388′ W	1068
L	26 Jan 2008	74°44.742′ S	164°10.816′ E	205
D	25 Jan 2008	75°07.994′ S	164°33.289′ E	1116
B	27 Jan 2008	73°59.158′ S	175°03.065′ E	578
G	27 Jan 2008	72°23.147′ S	173°03.393′ E	523
P	04 Feb 2008	70°53.212′ S	172°00.751′ E	2315

Calibration of temperature and conductivity sensors was performed before and after the cruise. Hydrological data were corrected and processed according to international procedures (UNESCO 1988). Standard algorithms (Fofonoff & Millard 1983) were used to compute derived quantities such as potential temperature, salinity and potential density anomaly.

The water samples that were used for the pH and the A_T analyses were collected from 12 L Niskin bottles and put into 500-mL borosilicate glass bottles, using the standard operating procedures described in the DOE handbook (DOE 2007a). The water samples were poisoned with saturated $HgCl_2$ solution to stop biological activity from altering the carbon distributions in the sample containers before analysis. Samples were stored in dark, cold ($+4°C$) conditions and analysed at the Department of Chemistry and Industrial Chemistry at the University of Genoa. The analyses were performed within four months of sampling.

Seawater A_T and pH measurements

The A_T (μmol kg^{-1} seawater) was measured using a potentiometric titration system with an 806 Exchange Unit (Metrohm, Herisau, Switzerland) and a 702 SM Titrino Dosimat (Metrohm, Herisau, Switzerland). We followed the methods described in the DOE handbook (DOE 2007a), which was adapted to our instrumentation (Rivaro, Messa et al. 2010).

Placed in an open cell, 165 g of seawater was titrated with a solution of hydrochloric acid (HCl) in a two-stage titration. The sample, maintained at constant temperature ($25 \pm 0.1°C$) using a thermostatic water bath, was first acidified to a pH of between 3.5 and 4.0 with a single aliquot of titrant (3.7 mL of HCl 0.1 M), then stirred for 10 min to allow for the liberation of the CO_2 that was evolved. The titration continued until a pH of about 3.0 was reached. The ionic strength of the HCl solution was adjusted with NaCl in order to be similar to that of the samples (salinity range 33.5–34.8). The progress of the titration was monitored using a pH glass electrode/reference electrode cell, and the A_T was computed from the titrant volume and potential difference measurements using a non-linear least-squares approach similar to that proposed in the DOE handbook (DOE 1994). The precision was computed from three replicate analyses of one sample at least daily and was determined to ± 3 μmol kg^{-1} ($\pm 0.1\%$). Routine analyses of Certified Reference Materials (batch no. 79, provided by A. G. Dickson, Scripps Institution of Oceanography) ensured the accuracy of the measurements, which was ± 3 μmol kg^{-1}.

The pH was expressed in the pH total scale, (i.e., $[H^+]$ as moles per kilogram of seawater, pH_T) and it was

determined using a potentiometric method that employed a combination glass/reference electrode with a negative temperature coefficient thermistor. The Tris-(hydroxymethyl)aminomethane (TRIS) buffer used to standardize the pH electrode was prepared according to the DOE handbook (DOE 2007b). The salinity of the TRIS buffer was 35. Both the TRIS buffer and the seawater samples were brought to the same temperature ($25 \pm 0.1^{\circ}C$) using a thermostatic water bath, before the measurements were conducted. The accuracy of the pH measure is strongly dependent on the composition of the TRIS buffer solution, but no certified material is currently available. Consequently, this figure of merit was not determined. The precision of the pH measurement was ± 0.007 units and was evaluated by repeated analysis of the A_T certified material. The pH_T measures at 25°C were then recalculated at in situ temperature and pressure conditions ($pH_{in\ situ}$).

pCO_2 and C_T calculation

A_T, pH_T, salinity and temperature were used as input parameters in the CO_2-chemical speciation model to calculate pCO_2 (CO_2SYS program [Pierrot et al. 2006]). We used the CO_2-system dissociation constants (K*1 and K*2) estimated by Roy et al. (1993), as a recent paper showed these constants to be the most suitable for cold and fresher surface waters (Chierici & Fransson 2009). We used the Dickson constant for the HSO_4^- (1990). Following Millero (2007), the estimated probable errors in the calculated parameters of the carbonate system using A_T and pH_T data as input measurements are ± 4 μmol kg^{-1} and ± 2 μatm, for both C_T and pCO_2, respectively.

Sea–air exchange of CO_2 and CO_2 flux formulation

The most direct method to estimate the uptake of atmospheric CO_2 by the oceans is by determining the air–sea flux from values of the pCO_2 in the sea surface and the overlying atmosphere. The net sea–air CO_2 exchange flux (F, mmol m^{-2} d^{-1}) is calculated using the formula:

$$F = ks(\Delta pCO_2), \quad (1)$$

where k is the CO_2 gas transfer velocity (cm h^{-1}), s is the solubility of CO_2 (mol kg^{-1} atm^{-1}) and ΔpCO_2 is the difference between the pCO_2 of the seawater (pCO_{2SW}) and the air (pCO_{2atm}). Negative ΔpCO_2 values indicate absorption of the gas by the sea surface, while positive values correspond to the release of the gas into the atmosphere. Therefore, the sea–air flux of CO_2 is dependent on the difference of CO_2 concentration between sea surface and atmosphere (ΔpCO_2, μatm) and proportional to the wind speed.

The ΔpCO_2 values were calculated as the difference between the pCO_2 in seawater, calculated from our A_T and pH measurements, and the atmospheric CO_2 mean value of 382 μatm available from the South Pole Observatory (http://www.esrl.noaa.gov/gmd/obop/spo/).

The atmospheric pCO_2 was corrected to 100% humidity at in situ sea-surface temperature (SST) and salinity (SSS). Correction for the water vapour pressure was carried out using the equations of Weiss & Price (1980). The water vapour pressure values were then used to correct $p(CO_2)$ dry to 100% humidity using the standard formula as given in DOE (1994) as Standard Operational Procedure 5.

The solubility coefficient *s* was calculated in each sample as a function of temperature (t) and salinity (S), using Weiss (1974). The gas transfer velocity k, depends on the wind speed *u*. We applied the Wanninkhof formulation (1992), where $k_{CO_2} = 0.31u^2\ (660/Sc_{CO_2})^{0.5}$ for instant wind speed measures or $k_{CO_2} = 0.39u^2\ (660/Sc_{CO_2})^{0.5}$ for averaged wind speed. We also applied the Wanninkhof & McGillis (1999) formulation where $k_{CO_2} = 0.0283u^3\ (660/Sc_{CO_2})^{0.5}$. Sc_{CO_2} is the Schmidt number for CO_2. We used our ship-based wind speed data at 10m height and monthly data provided by the European Centre for Medium-Range Weather Forecast (ECMWF) with a spatial resolution of $1^{\circ} \times 1^{\circ}$ for the grid points. The wind speeds used in this study are reported in Table 2.

Results

Physical characteristics of the water masses

Different water masses were identified in the sampled stations using potential temperature (θ), salinity (S) and neutral density (γ^n) values (Jackett & McDougall 1997) (Fig. 2; Table 3). Following Whitworth et al. (1998), Orsi et al. (1999) and Orsi & Wiederwohl (2009) we used the γ^n 28.00 kg m^{-3} and 28.27 kg m^{-3} values to separate the

Table 2 Wind speed used for CO_2 flux calculation in this study.

Station	Instantaneous shipboard wind speed (ms^{-1})	Monthly ECMWF[a] wind speed (ms^{-1})
A	4.1 ± 0.8	4.3 ± 3.4
H1	6.2 ± 1.2	7.3 ± 3.0
H2	1.5 ± 0.3	7.2 ± 3.2
H3	9.3 ± 1.8	7.1 ± 3.2
L	7.7 ± 1.5	4.4 ± 2.8
D	9.8 ± 1.9	4.8 ± 2.8
B	4.6 ± 0.9	7.2 ± 3.3
G	3.6 ± 0.7	7.6 ± 3.7
P	3.1 ± 0.6	9.2 ± 4.9

[a]European Centre for Medium-Range Weather Forecast.

Citation: *Polar Research* 2014, *33*, 20403, http://dx.doi.org/10.3402/polar.v33.20403

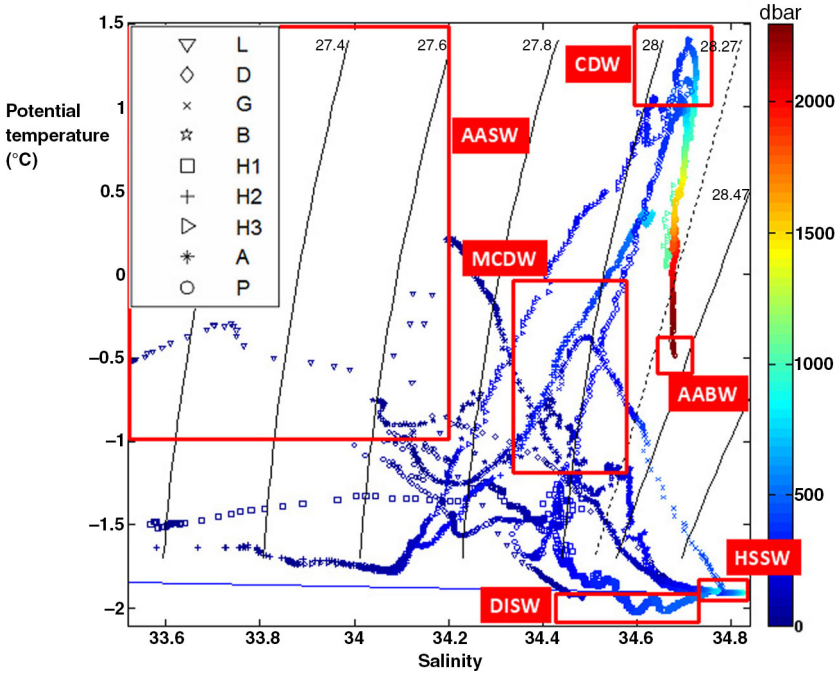

Fig. 2 Potential temperature salinity (θ/S) plot for the sampled stations. Major water masses are abbreviated as follows: Antarctic Surface Water (AASW), Circumpolar Deep Water (CDW) Modified Circumpolar Deep Water (MCDW), High Salinity Shelf Water (HSSW), Deep Ice Shelf Water (DISW) and Antarctic Bottom Water (AABW).

CDW from the AASW and from the densest water masses below, respectively. The six water masses that were identified are described below.

The AASW is characterized by a γ^n lower than 27.70 kg m^{-3} and by a wide range of temperatures (> -1.0°C) and salinities (< 34.20) due to its interaction with atmosphere and ice production and melting. Following the approach introduced by Mitchell & Holm-Hansen (1991) an increase of in situ density > 0.05 kg m^{-3} over 5 m depth interval was the criterion used to establish the depth of UML in the AAWS. A thin UML was found in TNBp (10–15 m), whereas it became thicker in the other stations, ranging from 23 m (station P) to 34 m (station H3). Our values are in agreement with those reported for the same areas by Massolo et al. (2009).

The CDW is characterized by a γ^n within the range of 28.00–28.27 kg m^{-3}, with a sharp core showing the temperature maximum (> 1.0°C).

The Modified Circumpolar Deep Water (MCDW), which is the CDW entering in the Ross Sea and isopycnally mixed with local water, is characterized by the same density range as CDW, but with lower temperatures.

The Deep Ice Shelf Water (DISW) is characterized by potential temperature below the surface freezing point (sfp) and present in front of the Ross Ice Shelf between 160°W and 180° (Orsi & Whiederwohl 2009).

The HSSW is characterized by a salinity maximum greater than 34.70, temperature near the sfp and by a γ^n greater than 28.60 kg m^{-3}.

The AABW is characterized always by a γ^n greater than 28.27 kg m^{-3} and with potential temperature below 0°C, which is found offshore the 700 m on the slope.

Table 3 Average values of physical properties for water masses found in the Ross Sea in 2008 survey.

Water mass	Temperature (°C)	Salinity	Neutral density (kg m^{-3})
AASW[a]	> -1.0	< 34.20	< 27.70
CDW[b]	> 1.0	$34.60 < S < 34.75$	$28.00 < \gamma^n < 28.27$
MCDW[c]	$-1.2 < T < 0.0$	$34.30 < S < 34.60$	$27.90 < \gamma^n < 28.20$
HSSW[d]	ca. Tsfp[g]	> 34.70	> 28.6
DISW[e]	$<$ Tsfp	> 34.45	> 28.4
AABW[f]	$-1.5 < T < -0.5$	> 34.60	> 28.27

[a]Antarctic Surface Water. [b]Circumpolar Deep Water. [c]Modified Circumpolar Deep Water. [d]High Salinity Shelf Water. [e]Deep Ice Shelf Water. [f]Antarctic Bottom Water. [g]Surface freezing point.

Distribution of the inorganic C parameters (A_T, pH, C_T and pCO_2)

The A_T measured in our samples ranged between 2275 and 2374 μmol kg^{-1} and had good agreement with previous data collected in the Ross Sea (Sandrini et al. 2007).

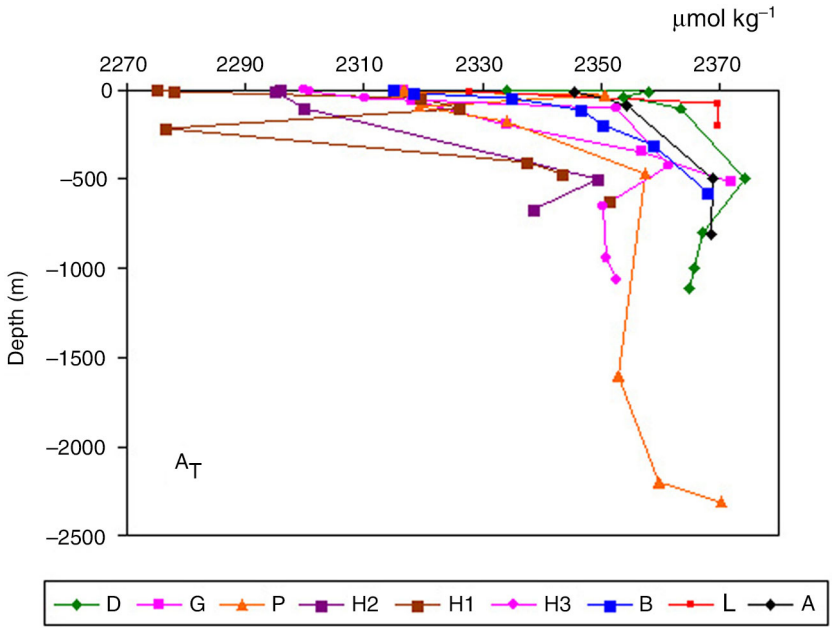

Fig. 3 Vertical profiles of the total alkalinity A_T in all of the sampled stations.

Figure 3 shows the A_T as a function of depth at all of the stations. Generally, the A_T profiles in the continental shelf stations had the lowest values in surface water (from 2275 to 2346 µmol kg^{-1}), an increasing gradient reaching the maximum values (from 2343 to 2374 µmol kg^{-1}) at ca. 500–700 m, and then lower values at deeper depths. The station P, sampled offshore, showed an increase in A_T values from ca. 1700 m to the deepest sampled depth (ca. 2300 m). At the surface, the highest values were measured at stations L, D and A (2328, 2334 and 2346 µmol kg^{-1}, respectively).

Pair-wise Pearson correlation coefficients were computed to examine the relationships between inorganic C parameters and hydrographic measurements. The A_T and the salinity were significantly and positively correlated (Pearson's $r = 0.86$, number of samples = 57), according to the following relationship:

$$A_T = 68.14S - 5.1804 \text{ µmol kg}^{-1} \quad (2)$$

No significant correlation were found between A_T and θ when the whole data set was considered. The relationship becomes significantly positive ($r = 0.62$, number of samples 16) when surface and subsurface samples (i.e., 1–10 m depth) are considered, suggesting that the temperature could explain some of the observed A_T variability in the AASW.

pH_T values recalculated at in situ temperature and pressure conditions ($pH_{in\ situ}$) ranged between 8.274 and 7.926. $pH_{in\ situ}$ was significantly and negatively correlated to S ($r = -0.71$) when the whole data set was considered. There was no correlation between $pH_{in\ situ}$ and either temperature or salinity when the 1–10 m depth samples were considered.

The $pH_{in\ situ}$ vertical distribution is shown in Fig. 4. The $pH_{in\ situ}$ has high and variable values in the surface layer (from 7.890 to 8.033 between 0 and ca. 100 m), then an abrupt drop with depth to approximately 100–400 m, followed by a slight increase and nearly constant values. At the surface, the lowest values were measured at stations H2, H3, G, B and P (8.108 ± 0.023), while stations D, L, A and H1 showed a higher variability and the highest pH values (8.186 ± 0.088). The same trend was observed in the subsurface layer too. An increasing gradient of the $pH_{in\ situ}$ can be observed from the offshore to the Ross Sea shelf stations, particularly at intermediate depths around 300–500 m. The left-most profile in Fig. 5 refers to station H3 sampled in the Glomar Challenger Trough (GCT; Fig. 1), where the absolute $pH_{in\ situ}$ minimum (7.950) was found in correspondence to the CDW intrusion. Comparable values were measured at station H2, sampled as well as station H3 in the GCT and at station P offshore the Drygalski Trough (DT; Fig. 1), the other well-known intruding area of the CDW in the Ross Sea.

The A_T, pH_T and the hydrographic data were used to calculate C_T and pCO_2. The C_T ranged from 2082 to 2263 µmol kg^{-1}; generally the lowest values were measured at the surface, with the absolute minimum at station H1, while the highest were measured at intermediate depths (ca. 500 m) at stations D, P, G, H3 and B. The C_T standard deviation in the AASW was higher than that

Citation: *Polar Research* 2014, *33*, 20403, http://dx.doi.org/10.3402/polar.v33.20403

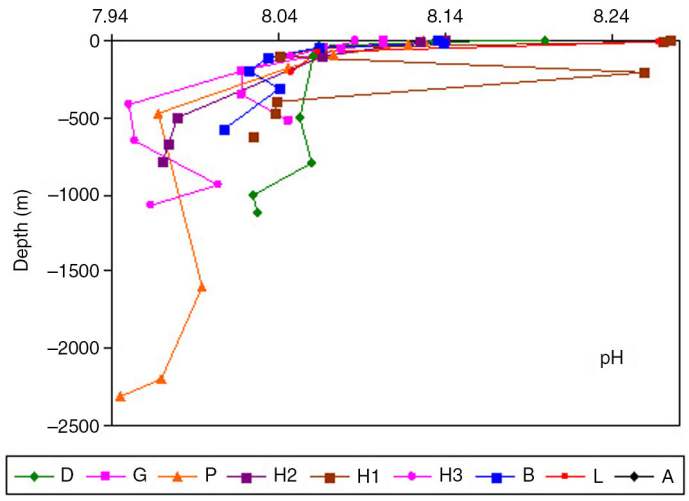

Fig. 4 profiles of the $pH_{in\ situ}$ in all of the sampled stations.

of A_T (39 vs. 23 µmol kg^{-1}), whereas in the intermediate and deep layers the standard deviations were comparable (6 vs. 5 µmol kg^{-1}, as mean values). The computed pCO_2 ranged from 207 to 479 µatm; the top of AASW (2–20 m) was undersaturated in CO_2 compared to calculated atmospheric values, particularly at stations L, D, A and H1, with pCO_2 varying between 207 and 338 µatm. The maxima were recorded at intermediate depths (ca. 500 m) at stations P and H3. The range of both parameters is in agreement with those reported for the Ross Sea waters (Sweeney 2003; Sandrini et al. 2007).

Discussion

Influence of sea ice and physical variables on the inorganic carbon parameters distribution in the AASW

The general vertical distribution of the inorganic carbon parameters (increasing for the A_T, the C_T and the pCO_2 and decreasing for pH) is mainly due to the biological activities (primary production and respiration, biogenic carbonate precipitation and dissolution), and to the physical properties of the water masses together with the

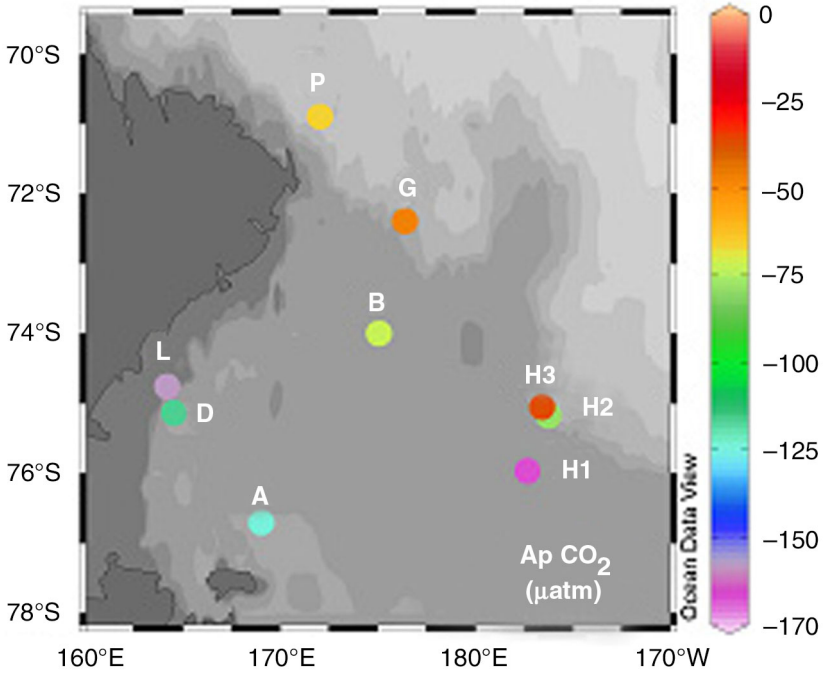

Fig. 5 ΔpCO_2 (pCO_{2SW}–pCO_{2air}) (µatm) calculated at the surface respect to a 382 ppm pCO_{2air}.

circulation pattern along the whole water column. The AASW occupies the top of the water column. The large standard deviation of the physical and chemical properties of AASW compared to the other water masses was consistent with the high variability of the upper layer of the water column, from the surface down to a depth of more than 100 m, which is strongly influenced by sea–ice–atmosphere interactions and by biological activity particularly in the summer season (when the sampling was performed).

Processes such as melting and formation of sea ice can play an important role in controlling the AASW physical features and inorganic carbon chemistry. In 2008, during the cruise, the sea-ice coverage was minimal and in the Ross Sea wide open sea areas were present (see satellite images at http://www.usap.gov/videoClipsAndMaps). Solar heating and decreased salinity, due to pack-ice melting, were responsible for the formation of the shallow UML in the AASW. To evaluate any effect of the sea-ice melting on the A_T and C_T distribution at the surface, following Rivaro et al. (2011), we calculated the meltwater percentage (MW%), considering the difference between the salinity measured at the surface (S_{meas}) and the salinity measured in the same station at greater depth (S_{deep}), which was not influenced by sea-ice dilution, assuming an average sea-ice salinity of 6 (Ackley et al. 1979):

$$MW\% = \left(1 - \frac{S_{meas} - 6}{S_{deep} - 6}\right) * 100. \quad (3)$$

In our study, S_{deep} depths were chosen on the basis of their γ^n values; that is, we chose samples collected below the γ^n 28.00 kg m^{-3}, which is the lower boundary of the AASW (Table 4).

MW% ranged from 1.1 (station P) to 4.1 (station A); the stations sampled in the GCT (H1, H2, H3) had ca. 3% MW, while stations L and D, sampled at TNBp had 1.2 and 1.8 MW%, respectively. The 2008 MW% fell into the range of values observed in 2006, which was considered as a standard year for sea-ice coverage in the Ross Sea shelf area (Massolo et al. 2009). The highest MW% calculated for stations H1, H2, H3 was consistent with the sea-ice coverage shown by satellite maps before the sampling period, showing a higher pack-ice extension in the GCT than in the polynya area. The MW% co-varied significantly and negatively with A_T (Pearson's $r = -0.79$, $P = 0.05$) and C_T (Pearson's $r = -0.62$, $P = 0.05$). This is consistent with the fact that the distribution of surface A_T and C_T is controlled by the factors that govern salinity. Therefore, the addition of sea-ice meltwater, which has low salinity, results in a dilution of the A_T and C_T. Unlike C_T, pH and pCO_2, photosynthesis and oxidation of organic matter have little direct influence on A_T (Redfield et al. 1963). Calcifying organisms can influence A_T and C_T concentration, but it is well known that the phytoplankton in the southern Ross Sea is dominated by two taxa that are spatially distinct: *Fragilariopsis curta*, a pennate diatom, dominating the coastal region, and *P. antarctica*, a colonial prymnesiophyte, dominating the south central region (Smith & Nelson 1985; Smith et al. 1996; Arrigo et al. 1999). Both are not calcifying organisms and therefore they are not able to influence A_T and C_T. Gordon et al. (2000) also reported that A_T does not vary during the summer in the Ross Sea, suggesting that phytoplanktonic calcifying organisms are unimportant in the carbon cycle in this region.

A correlation between the surface A_T and temperature values was found in our study, suggesting that the temperature could explain some of the A_T variability, consistent with the dependence found for surface waters of the world ocean. In particular, Lee et al. (2006) proposed several relationships to estimate A_T from salinity and temperature surface measurements. We applied the relationship proposed for the Southern Ocean to our data set:

$$A_T = 2305 + 52.48(SSS - 35) + 2.85(SSS - 35)^2 - 0.49(SST - 20) + 0.086(SST - 20)^2, \quad (4)$$

where SSS and SST are sea-surface salinity and temperature, respectively.

This relationship gave poor results, because the analysis of the residual, which is a good measure of the accuracy of the predictivity of the curve fitting, was about 11 μmol kg^{-1}, higher than the accuracy of our measurements (3 μmol kg^{-1}). Afterwards, a new similar relationship that provided more accurate estimates of A_T from the measured SSS and SST for the surface waters of the Ross Sea was found. To find the new relationship we used the surface samples collected during the 2003 Climatic Long Term

Table 4 Data used for melt water percentage (MW%) calculation.

Station	S_{meas}	S_{deep}	Depth (m) S_{deep}	Corresponding γ^n (kg m^{-3})	Calculated MW%
A	34.20	34.53	85	28.08	1.2
H1	33.59	34.45	250	28.01	3.0
H2	33.80	34.57	500	28.02	2.7
H3	33.90	34.71	420	28.05	2.8
L	33.53	34.70	75	28.64	4.1
D	34.19	34.71	100	28.66	1.8
B	34.08	34.501	110	28.07	1.5
G	34.14	34.59	230	28.05	1.6
P	34.07	34.39	180	28.01	1.1

Citation: *Polar Research* 2014, *33*, 20403, http://dx.doi.org/10.3402/polar.v33.20403

Interaction for the Mass-balance in Antarctica (CLIMA) cruise ($n = 82$; Sandrini et al. 2007). The results were:

$$A_T = 2308 + 108.98(SSS - 34) + 60.70(SSS - 34)^2 + (-6.91[SST + 1.30]) + 9.091(SST + 1.30)^2 \quad (5)$$

Equation 5 was then applied to our samples; the analysis of the residual was 4 μmol kg^{-1}, confirming its validity for the Ross Sea and showing that we could estimate the A_T from SSS and SST in the Ross Sea AASW with a precision comparable to our measurements.

The variability of the $pH_{in\ situ}$ in the surface layer can be ascribed primarily to biological production and vertical mixing. Primary production increases the pH of seawater as a result of the displacement of the carbonate equilibrium related to CO_2 consumption, while the vertical mixing of the surface water with deeper water causes a decrease of the pH. The correlation between $pH_{in\ situ}$ and S or θ was not significant in the AASW samples, suggesting that physical variables do not have a strong direct influence on the distribution of this parameter at the surface, which is therefore mainly governed by biological processes. The $pH_{in\ situ}$ was negatively and significantly correlated to C_T, while it was not correlated with A_T. The highest values were observed in stations D, H1 and A, which coincided with low C_T values (2161, 2082 and 2158 μmol kg^{-1}, respectively) and a slightly higher A_T:C_T ratio (1.09), suggesting that C_T plays a more significant role in regulating pH than A_T. The exchanges of CO_2 with the atmosphere can result in a modification of pH as well, but this effect is weak over the short time scale that we investigated.

Sea-air CO_2 fluxes

All pCO_2 values of the surface and subsurface waters (2–20m) were below atmospheric levels, particularly at stations L, D, A and H1, with pCO_2 varying between 207 and 338 μatm. Considerable variation was, however, observed spatially (Table 5). Consequently, the ΔpCO_2 (pCO_{2SW}–pCO_{2air}) was negative (from −44 to −175 μatm), outlining that the Ross Sea was a potential sink for CO_2 during the sampling (Fig. 5). In surface seawater the pCO_2 depends on SST, SSS, C_T and A_T concentrations. These determinants are influenced by several processes such as warming/cooling and biological activity (Bellerby et al. 2004). Even though the pCO_2 is influenced by the SST and SSS, no relationship between pCO_2 and physical variables was found in our samples collected in the surface waters. This agrees with the results obtained by Poisson et al. (1993) and Metzl et al. (1999), who did not find a large-scale correlation between fCO_2 and SST in the Southern Ocean during the austral summer. Laika et al. (2009) confirmed that biological effects dominate the temperature effect on the pCO_2 distribution, especially in the areas south of the Polar Frontal Zone, from the Permanent Open Ocean Zone to the Antarctica shelf areas. The Ross Sea is one of the most productive areas of the Southern Ocean. Marginal ice zones and polynyas are often associated with high primary productivity, which is the result of higher light availability (due to the reduced sea-ice cover) and higher micronutrient availability (in particular, Fe; Tagliabue & Arrigo 2006). The RSp (Fig. 1) is the most productive polynya, but the TNBp, which is smaller than the RSp, is also important in terms of productivity (Mangoni et al. 2004). The phytoplankton bloom develops later in the year at the TNBp compared to RSp and it is dominated by diatoms. Phytoplankton abundance is maximal in late December, declines thereafter, but a secondary peak appears in mid-February (Tremblay & Smith 2007). In our survey, the highest pCO_2 drawdown was calculated in the TNBp and RSp and in station H1, which was sampled in a marginal ice area. Unfortunately, we could not directly confirm the

Table 5 Surface temperature, salinity, pCO_2 and ΔpCO_2 together with the mean values and the standard deviations calculated for the fluxes of CO_2.

Station	T°C	S	pCO_2 (μatm)	ΔpCO_2 (μatm)	Flux CO_2^a (mmol $m^{-2}d^{-1}$)	Flux CO_2^b (mmol $m^{-2}d^{-1}$)	Flux CO_2^c (mmol $m^{-2}d^{-1}$)
A	+0.151	34.20	251	−131	−2.8±0.5	−3.8±2.8	−1.2±0.9
H1	−1.566	33.59	207	−175	−9.0±1.7	−15.3±6.0	−8.2±3.2
H2	−1.65	33.80	296	−86	−0.3±0.1	−7.4±2.9	−3.9±1.5
H3	−1.745	33.90	338	−44	−5.0±0.8	−3.6±1.4	−1.9±0.7
L	−0.309	33.53	216	−166	−12.7±2.4	−5.2±3.1	−1.7±1.0
D	−0.863	34.19	258	−125	−15.4±2.9	−4.5±2.4	−1.6±0.9
B	−0.752	34.08	304	−79	−2.2±0.4	−6.5±2.7	−3.4±1.4
G	−0.989	34.14	328	−54	−0.9±0.1	−5.0±2.1	−2.8±1.2
P	−1.155	34.07	309	−73	−0.9±0.1	−9.9±4.7	−6.6±3.1

[a]Flux calculated following Wanninkhof (1992), using $k_{CO_2} = 0.32u^2$ $(660/Sc)^{0.5}$ and instantaneous shipboard wind speed data. [b]Flux calculated following Wanninkhof (1992), using $k_{CO_2} = 0.39u^2$ $(660/Sc)^{0.5}$ and monthly data provided by the European Centre for Medium-Range Weather Forecast. [c]Flux calculated following Wanninkhof & McGillis (1999), using $k_{CO_2} = 0.0283u^3$ $(660/Sc)^{0.5}$ and monthly data provided by the European Centre for Medium-Range Weather Forecast.

phytoplanktonic drawdown on the pCO_2, distribution, because neither chlorophyll-a sampling nor fluorescence measurements were performed. Nevertheless, primary productivity calculated from Sea WiFS data referred to the investigated period (available at http://giovanni.gsfc.nasa.gov) and the comparison with data collected in previous surveys allowed us to hypothesize that the phytoplanktonic drawdown made an important contribution in determining the pCO_2 in the upper AAWS (Bates et al. 1998; Gordon et al. 2000; Sweeney et al. 2000; Takahashi et al. 2002; Barbini et al. 2003; Sweeney 2003; Arrigo & Van Dijken 2007). In particular, Barbini et al. (2003) correlated the phytoplanktonic bloom events with the high chlorophyll-a concentrations and low pCO_2 values measured in selected sites during the XVI Italian Expedition (austral summer 2000–01) such as TNBp (corresponding with stations D and L), the RSp near Ross Island (corresponding with station A), and in the central basin area (corresponding with station H) (Fig. 1). Conversely, high values of surface pCO_2 were encountered towards the northern margin of the Ross Sea shelf area above 73°S latitude, in the offshore area near Cape Adare and Cape Hallet where stations G and P were sampled in our survey (Fig. 1). Other evidence corroborating the hypothesis that primary production was playing an important role in regulating CO_2 distribution in the Ross Sea during austral summer 2008, could come from our O_2 measurements (data not shown). The O_2 concentration was compared with oxygen saturation (calculated from S and T) and a disequilibrium in O_2 was observed in TNBp and RSp. The undersaturation in CO_2 coincided with a supersaturation in O_2, which could not be explained by a change in the hydrography. Finally, the pCO_2 and the $pH_{in\ situ}$ correlated negatively and significantly in the AASW, consisting with the increase of the pH due to primary production as a result of the displacement of the carbonate equilibrium related to CO_2 consumption.

The sea–air fluxes of CO_2 were calculated (Table 5). Wind speed is the main driver of the air—sea flux, together with the ΔpCO_2. Both wind speed data (shipboard and ECMWF data) used to calculate the kCO_2 showed a marked spatial variation (Table 2), which greatly influenced the calculated CO_2 fluxes. Since the relationship between u and kCO_2 is still a source of uncertainty, we have applied different formulations. As a consequence of the negative ΔpCO_2 values, the air—sea CO_2 fluxes were directed towards the water column and no upward CO_2 flux was calculated. Significant variability in the CO_2 sea–air flux was observed, with mean values ranging from -0.3 to -15.4 mmol m^{-2} d^{-1}. Although the differences, resulting from the choice of exchange coefficient and the chosen non-linear relationships between wind speed and gas transfer velocity were large, our range is comparable to those calculated by Bates et al. (1998) and Sweeney et al. (2000), who used long-term average wind speeds. The large flux uncertainty comes from the error in ΔpCO_2, the errors in the scaling factor for the gas transfer rate formula and the wind speed variability. Using shipboard wind data, the highest mean flux was calculated at station D, where high drawdown of CO_2 by biological activity was supposed. Using ECMWF wind data (lower than shipboard data; Table 2), the estimated flux resulted in being three times lower. When fluxes were calculated using the cubic relationship between wind speed and CO_2 flux, the sink observed at TNBp became even weaker. In any case, it is important to note that our estimates are a snapshot only, describing the situation that we found during our cruise so that the mean fluxes should only be taken as indicative; therefore, any extrapolation to a seasonal flux should be treated carefully.

Influence of water masses and circulation pattern on distribution of inorganic carbon parameters in Ross Sea shelf area

On the basis of the thermohaline properties and γ^n values, several intermediate and deep-water masses were identified in this study. Afterwards, the values of the chemical parameters were constrained by the physical values used to differentiate the local water masses. Differently from AASW, the physical and chemical properties varied within a relatively narrow range.

CDW is a relatively warm and salty water mass that originates in the Antarctic Circumpolar Current (ACC) and episodically intrudes into the Ross Sea on the shelf, forced by the curvature of the bathymetry (Dinniman et al. 2003). On the shelf, isopycnal mixing with cold and low-salinity AASW rapidly attenuates the characteristics of the CDW offshore, producing MCDW (Jacobs & Giulivi 1999). CDW or MCDW is thought to be important to many processes, such as the formation of AABW (Orsi et al. 1999; Gordon, Orsi et al. 2009; Orsi & Wiederwohl 2009), the dynamics of the RSp (Reddy et al. 2007), and supplying much of the heat involved in the basal melting of the Ross Ice Shelf (Smethie & Jacobs 2005). CDW contains low levels of O_2 and high levels of nutrients (nitrate, NO_3, phosphate PO_4 and silicate $Si(OH)_4$) and of C_T, as it has an older ventilation age compared to the recently formed SW (Rivaro et al. 2004; Sandrini et al. 2007; Rivaro, Massolo et al. 2010).

The mid-depth (ca. 500 m) intrusion of the CDW and its modification in MCDW was traced over the shelf by the high θ, C_T and pCO_2 values (> -0.8°C, 2251 ± 7 μmol kg^{-1} and 463 ± 14 μatm, respectively) and by the

Citation: *Polar Research* 2014, *33*, 20403, http://dx.doi.org/10.3402/polar.v33.20403

low $pH_{in\ situ}$ (7.969 ± 0.025), particularly at stations P and H3 (Fig. 5). These stations were located along the slope in the two well documented sites of CDW intrusion in the Ross Sea shelf area, the DT and the GCT, respectively (Orsi & Whiederwool 2009). The re-mineralization of organic matter consumes O_2, further increasing the nutrient, C_T and pCO_2 concentrations. The pH decreases due to the addition of CO_2 from the oxidation of organic carbon. The high C_T and the low $pH_{in\ situ}$ characterizing the CDW are consistent with the old ventilation time, the low O_2 and the high nutrient values. For this last feature, the intrusion of CDW on the shelf could represent a source of nutrients for biological production.

The HSSW is defined by $\gamma^n > 28.60$ kg m^{-3}, S > 34.70 and temperatures close to the sfp; it is formed along Victoria Land and mainly in the TNBp area by brine rejection during surface water freezing and the strong katabatic winds flowing down to the Antarctic plateau (Budillon & Spezie 2000). The HSSW spreads northward along the DT, where it reaches the shelf break and ventilates the deep ocean producing AABW. Another branch moves southward beneath the Ross Ice Shelf taking part in the production of the DISW (Jacobs et al. 1985). DISW is defined by $\gamma^n = 28.40$ kg m^{-3}, salinity higher than 34.45 and temperatures close to the sfp. The DISW core moves northward along the GCT, reaching the shelf break near 75°S close to the dateline meridian where it also mixes with the intruding CDW taking part in AABW production (Budillon et al. 2003; Rubino et al. 2003; Smethie & Jacobs 2005; Budillon et al. 2006). Both HSSW and DISW are characterized by high O_2 concentrations (about 295 μM), reflecting the origin of AASW in the case of HSSW and the contribution of glacial meltwater in the case of DISW. The HSSW was characterized by the A_T maxima (2367 ± 6 μmol kg^{-1}), measured in the entire water column below 100–200 m in the D and L stations in the layers deeper than 500 m in the A, H1, B and G stations, which were sampled in correspondence to the preferential pathways of the spreading HSSW. The high correlation between A_T and S and the conservative behaviour justify the fact that the highest A_T values are found in the deeper layers of the water column measured at stations L and D sampled at TNBp, which is the main site of HSSW production in the Ross Sea.

The DISW was identified by θ and S values at intermediate depths (between 400 and 500 m) in H1, and it was characterized by lower A_T than the HSSW (2341 ± 4 μmol kg^{-1}). This difference is due to the dilution effect produced by glacial meltwater addition in the DISW production. Therefore, the A_T adds some information to the chemical characterization of the water masses, being able to chemically trace the two water masses. The same feature is shown by C_T too; that is, HSSW has a C_T higher than DISW (2251 ± 8 and 2228 ± 3, respectively). Taking into account that both SWs take part in the Ross Sea AABW production, and the role played by AABW as a CO_2 sink we can suppose that the plume produced in the DT injects a higher C_T into the deep ocean than the plume leaving the GCT.

According to the definition by Orsi & Wiederwohl (2009), the AABW lies on the slope at depth >700 m, it is always characterized by a γ^n greater than 28.27 kg m^{-3} and by θ < 0°C. In our data set these characteristics were shown by the deepest layers (depth > 1850 m) at station P only, sampled in the DT mouth. No AABW was identified in the samples collected in the GCT, although this area is a well-known AABW production site as documented by several CTD and moored station measurements (Smethie & Jacobs 2005; Budillon et al. 2011). In fact the deepest layers of station H3, (depth > 700 m) do not have θ < 0°C and $\gamma^n > 28.27$ kg m^{-3} (Fig. 2, Table 3). For this reason, we cannot evaluate whether the AABW produced in the two regions of the Ross Sea contains different amounts of C_T and as a consequence whether the plume produced in the DT injects a higher C_T into the deep ocean than the plume leaving the GCT.

The precipitation or formation of solid $CaCO_3$ in surface waters and the dissolution of solid $CaCO_3$ in deep waters can be important in transferring CO_2 from surface to deep waters. The uptake of CO_2 by surface layers increases the concentration of H^+, which lowers pH and, in changing the chemical equilibrium of the inorganic carbon system, reduces the concentration of CO_3^{2-}. Carbonate ions are required by marine calcifying organisms such as plankton, shellfish and fish to produce calcium carbonate shells and skeletons.

The saturation state of the seawater with respect to $CaCO_3$ is expressed by the ratio

$$\Omega = [Ca^{2+}][CO_3^{2-}]/K'_{sp}, \quad (6)$$

where $[Ca^{2+}][CO_3^{2-}]$ is the ion product of the concentration of calcium and carbonate ions, and K'_{sp} is the solubility product depending on in situ temperature, salinity and pressure and on the particular mineral phase (aragonite is approximately 50% more soluble than calcite [Mucci 1983]). The values of $[CO_3^{2-}]$ and of Ω have been determined from A_T and pH, using the CO_2SYS program. All of the samples were oversaturated with respect both to the calcite and to the aragonite, with the exception of the deepest layers (below 1600 m) of P station, which were undersaturated with respect to the aragonite. Near corrosive levels of aragonite saturation state (Ω_{arag}) (Ω ca. 1.1–1.2) were found in correspondence to the entrainment of CDW both in the DT and in

the GCT. Our data are in agreement with Ω_{arag} and pH values and variability in the Ross Sea calculated by McNeil et al. (2010). It has been predicted that the Southern Ocean will become undersaturated with respect to aragonite by 2030 (McNeil & Matear 2008). The onshore transport of CDW, whether sporadic and occurring only at specific locations, could accelerate the Ross Sea acidification process, with respect to these predictions. Aragonite undersaturation is of particular concern for the zooplankton species comprising pteropods, which form aragonite shells. In fact, pteropods comprise up to one-quarter of the total zooplankton biomass in the Ross Sea (Hopkins 1987). Recently, Manno et al. (2007) described the occurrence of initial dissolution of the aragonitic shells of the pteropod *Limacina helicina* above the saturation depth in the TNBp area, while Honjo (2004) reported pteropod shell degradation at a depth of 1 km and below south of the Polar Front Zone. Bednaršek et al. (2012) comparing the shell structure of specimens *L. helicina,* that were extracted live from the Southern Ocean, with samples from aragonite-supersaturated regions, found severe levels of shell dissolution in the Southern Ocean organisms. All of these results suggest that changes in carbonate chemistry in the water column are already occurring and that they could possibly have significant effects throughout the Ross Sea marine food web.

Conclusion

Given the role of the Ross Sea in the global carbon budget, better knowledge of its inorganic carbon properties is required. This work presents the distribution of A_T and pH based on the hydrochemical data collected in the Ross Sea shelf area during February 2008. Our measurements represent a contribution to the current understanding of carbonate chemistry in the Ross Sea, and provide insights into the biogeochemical processes that are occurring and the potential changes which may be reasonably expected in the near future. The influence of the sea ice and of the physical properties of the seawater on the inorganic carbon parameters distribution in the AASW was observed. In the deep layers of the water column, the A_T maxima were measured in correspondence to the preferential pathways of the spreading HSSW. Moreover, the A_T which is strongly dependent on salinity allowed us to chemically trace the HSSW and to distinguish it from DISW.

The pH was not significantly correlated to physical variables in the surface waters, where the pH variations are mainly governed by biological processes. At mid-depths (300–500 m) a decreasing pH gradient was observed from the shelf area to offshore, in correspondence with the CDW intrusion, where near corrosive level of aragonite saturation state (Ω ca. 1.1–1.2) were found.

Furthermore, our results, despite the uncertainties and assumptions involved, showed that during our survey the Ross Sea acted as a sink for atmospheric CO_2 with a large variability, depending on biological activity and wind speed.

Climate change feedbacks such as ocean warming, deep-water ventilation changes, and sea-ice melt potentially alter future ocean carbonate conditions found in this study both in the surface and the deep layers of the Ross Sea with some consequences on the role of the AABW in the export of inorganic carbon, particularly in the capture of the anthropogenic CO_2. Therefore, further investigations in the Ross Sea are necessary to confirm the findings to date and to investigate the temporal evolution of the carbonate system properties.

Acknowledgements

This study was carried out as part of the PNRA CLIMA and Terranova bay Research Experiment (T-REX) projects and was funded by the Italian National Agency for New Technologies, Energy and Sustainable Economic Development through a joint research programme. The help of the crew on the RV *Italica* is kindly acknowledged. The authors are grateful to Prof. G.L. Gragnani (University of Genoa) for the calculation performed by GnuPlot software. SeaWIFS analyses and visualizations used in this paper were produced with the Giovanni online data system, developed and maintained by the National Aeronautics and Space Administration's Goddard Earth Sciences Data and Information Services Center. We thank Novilinguists Multimedia for the English editing. The comments and the suggestions of the referees were greatly appreciated and improved this paper.

References

Ackley S.F., Buck K.R. & Taguchi S. 1979. Standing crop of algae in the sea ice of Weddell Sea region. *Deep-Sea Research Part I 26*, 269–281.

Arrigo K.R., Robinson D.H., Worthen D.L., Dumbar R.B., Di Tullio G.R., Van Woerth M. & Lizotte M.P. 1999. Phytoplankton community structure and the drawdown of nutrient and CO_2 in the Southern Ocean. *Science 283*, 365–367.

Arrigo K.R. & Van Dijken G.L. 2004. Annual changes in sea-ice, chlorophyll-a, and primary production in the Ross Sea, Antarctica. *Deep-Sea Research Part II 51*, 117–138.

Arrigo K.R. & Van Dijken G.L. 2007. Interannual variation in sea–air CO_2 flux in the Ross Sea, Antarctica: a model

Citation: *Polar Research* 2014, *33*, 20403, http://dx.doi.org/10.3402/polar.v33.20403

analysis. *Journal of Geophysical Research—Oceans 112*, 03020, doi: 10.1029/2006JC003492.

Barbini R., Fantoni R., Palucci A., Colao F., Sandrini S., Ceradini S., Tositti L., Tubertini O. & Ferrari G.M. 2003. Simultaneous measurements of remote lidar chlorophyll and surface CO_2 distributions in the Ross Sea. *International Journal of Remote Sensing 24*, 3807–3819.

Bates N.R., Hansell D.A. & Carlson C.A. 1998. Distribution of CO_2 species, estimates of net community production, and sea–air CO_2 exchange in the Ross Sea polynya. *Journal of Geophysical Research—Oceans 103*, 2883–2896.

Bednaršek N., Tarling G.A., Bakker D.C.E., Fielding S., Jones E.M., Venables H.J., Ward P., Kuzirian A., Lézé B., Feely R.A. & Murphy E.J. 2012. Extensive dissolution of live pteropods in the Southern Ocean. *Nature Geoscience 12*, 881–885.

Bellerby R.G.J., Hoppema M., Fahrbach E., De Baar H.J.W. & Stoll M.H.C. 2004. Interannual controls on Weddell Sea surface water fCO_2 during the autumn–winter transition phase. *Deep-Sea Research Part I 51*, 793–808.

Bromwich D.A., Parish T.R. & Zorman C.A. 1990. The confluence zone of the intense katabatic winds at Terra Nova Bay, Antarctica, as derived from airborne sastrugi surveys and mesoscale numerical modelling. *Journal of Geophysical Research—Atmospheres 95*, 5495–5509.

Budillon G., Castagno P., Aliani S. & Spezie G. 2011. Thermohaline variability and Antarctic bottom water formation at the Ross Sea shelf break. *Deep-Sea Research Part I 58*, 1002–1018.

Budillon G., Pacciaroni M., Cozzi S., Rivaro P., Catalano G., Ianni C. & Cantoni C. 2003. An optimum multiparameter mixing analysis of the shelf waters in the Ross Sea. *Antarctic Science 15*, 105–118.

Budillon G., Salusti E. & Tucci S. 2006. The evolution of density currents and nepheloid bottom layers in the Ross Sea (Antarctica). *Journal of Marine Research 64*, 517–540.

Budillon G. & Spezie G. 2000. Thermohaline structure and variability in the Terra Nova Bay Polynya (Ross Sea) between 1995–98. *Antarctic Science 12*, 501–516.

Caldeira K. & Duffy P.B. 2000. The role of the Southern Ocean in uptake and storage of anthropogenic carbon dioxide. *Science 287*, 620–622.

Chierici M. & Fransson A. 2009. $CaCO_3$ saturation in the surface water of the Arctic Ocean: undersaturation in freshwater influenced shelves. *Biogeosciences 6*, 2421–2432.

Dickson A.G. 1990. Standard potential of the reaction: $AgCl(s) + 1/2\ H_2(g) = Ag(s) + HCl(aq)$, and the standard acidity constant of the ion HSO_4^- in synthetic seawater from 273.15 to 318.15 K. *Journal of Chemical Thermodynamics 22*, 113–127.

Dinniman M.S., Klinck J.M. & Smith W.O. Jr. 2003. Cross-shelf exchange in a model of the Ross Sea circulation and biogeochemistry. *Deep-Sea Research Part II 50*, 3103–3120.

DOE (US Department of Energy) 1994. *Handbook of methods for the analysis of the various parameters of the carbon dioxide system in sea water. Version 2.0. ORNL/CDIAC-74*. A.G. Dickson & C. Goyet (eds.). Accessed on the internet at http://cdiac.esd.ornl.gov/oceans on 03 October 2014.

DOE (US Department of Energy). 2007a. *Handbook of methods for the analysis of the various parameters of the carbon dioxide system in sea water. Version 2.0. ORNL/CDIAC-74*. A.G. Dickson & C. Goyet (eds.). Accessed on the internet at http://cdiac.esd.ornl.gov/oceans on 29 August 2014.

DOE (US Department of Energy) 2007b. *Handbook of methods for the analysis of the various parameters of the carbon dioxide system in sea water. Version 3.0*. A.G. Dickson & C. Goyet (eds.). Accessed on the internet at http://cdiac.esd.ornl.gov/oceans on 29 August 2014.

Feng Y., Hare C.E., Rose J.M., Handy S.M., Di Tullio G.R., Lee P.A., Smith W.O. Jr., Peloquin J., Tozzi S., Sun J., Zhang Y., Dunbar R.B., Long M.C., Sohst B., Lohan M. & Hutchins D.A. 2010. Interactive effects of iron, irradiance and CO_2 on Ross Sea phytoplankton. *Deep-Sea Research Part I 57*, 368–383.

Fofonoff P. & Millard R.C. 1983. *Algorithms for computation of fundamental properties of seawater. UNESCO Technical Papers in Marine Science 44*. Paris: United Nations Educational, Scientific and Cultural Organization.

Fusco G., Budillon G. & Spezie G. 2009. Surface heat fluxes and thermohaline variability in the Ross Sea and in Terra Nova Bay polynya. *Continental Shelf Research 29*, 1887–1895.

Garrison D.L., Gibson A., Kunze H., Gowing M.M., Vickers C.L., Mathot S. & Bayre R.C. 2003. The Ross Sea polynya project: diatom- and *Phaeocysis*-dominated phytoplankton assemblages in the Ross Sea, Antarctica, 1994–1996. In G. Di Tullio & R.B. Dunbar (eds.): *Biogeochemistry of the Ross Sea*. Pp. 53–76. Washington DC: American Geophysical Union.

Gordon A.L., Orsi A.H., Muench R., Huber B.A., Zambianchi E. & Visbeck M. 2009. Western Ross Sea continental slope gravity currents. *Deep-Sea Research Part II 56*, 796–817.

Gordon A.L., Padman L. & Bergamasco A. 2009. Southern Ocean shelf slope exchange. *Deep-Sea Research Part II 56*, 775–777.

Gordon L.I., Codispoti L.A., Jennings J.C. Jr., Millero F.J., Morrison J.M. & Sweeney C. 2000. Seasonal evolution of hydrographic properties in the Ross Sea, Antarctica, 1996–1997. *Deep-Sea Research Part II 47*, 3095–3117.

Honjo S. 2004. Particle export and the biological pump in the Southern Ocean. *Antarctic Science 16*, 501–516.

Hopkins T.L. 1987. Midwater food web in McMurdo Sound, Ross Sea, Antarctica. *Marine Biology 89*, 197–212.

Jacobs S.S., Fairbanks R.C. & Horibe Y. 1985. Origin and evolution of water masses near the Antarctic continental margin: evidence from $H_2^{18}O/H_2^{16}O$ ratios in seawater. *Antarctic Research Series 43*, 59–85.

Jacobs S.S. & Giulivi C.F. 1999. Thermohaline data and ocean circulation on the Ross Sea continental shelf. In G. Spezie & G.M.R. Manzella (eds.): *Oceanography of the Ross Sea, Antarctica*. Pp. 3–16. Berlin: Springer.

Jackett R. & McDougall T.J. 1997. A neutral density variable for the world's oceans. *Journal of Physical Oceanography 27*, 237–263.

Laika H.E., Goyet C., Vouve F., Poisson A. & Touratier F. 2009. Interannual properties of the CO_2 system in the Southern Ocean south of Australia. *Antarctic Science 21*, 663–680.

Lee K., Tong L.T., Millero F.J., Sabine C.L., Dickson A.G., Goyet C., Park G.H., Wanninkhof R., Feely R.A. & Key R.M. 2006. Global relationships of total alkalinity with salinity and temperature in surface waters of the world's oceans. *Geophysical Research Letters 33*, L19605, doi: 10.1029/2006GL027207.

Mangoni O., Modigh M., Conversano F., Carrada G.C. & Saggiomo V. 2004. Effects of summer ice coverage on phytoplankton assemblages in the Ross Sea, Antarctica. *Deep-Sea Research Part I 5*, 1601–1617.

Manno C., Sandrini S., Tositti L. & Accornero A. 2007. First stages of degradation of *Limacina helicina* shells observed above the aragonite chemical lysocline in Terra Nova Bay (Antarctica). *Journal of Marine System 68*, 91–102.

Massolo S., Messa R., Rivaro P. & Leardi R. 2009. Annual and spatial variations of chemical and physical properties in the Ross Sea surface waters (Antarctica). *Continental Shelf Research 29*, 2333–2344.

McNeil B.I. & Matear R. 2008. Southern Ocean acidification: a tipping point at 450 ppm atmospheric CO_2. *Proceedings of the National Academy of Sciences of the United States of America 105*, 18860–18864.

McNeil B.I., Tagliabue A. & Sweeney C. 2010. A multi-decadal delay in the onset of corrosive 'acidified' waters in the Ross Sea of Antarctica due to strong sea–air CO_2 disequilibrium. *Geophysical Research Letters 37*, L19607, doi: 10.1029/2010GL044597.

Metzl N., Tilbrook B. & Poisson A. 1999. The annual fCO_2 cycle and the air–sea CO_2 flux in the sub-Antarctic Ocean. *Tellus Series B 51*, 849–861.

Millero F. 2007. The marine inorganic carbon cycle. *Chemical Reviews 107*, 308–341.

Mitchell B.G. & Holm-Hansen O. 1991. Observation and modelling of the Antarctic phytoplankton crop in relation to mixing depth. *Deep-Sea Research Part I 38*, 981–1007.

Mucci A. 1983. The solubility of calcite and aragonite in seawater at various salinities, temperatures, and one atmosphere total pressure. *American Journal of Science 283*, 780–799.

Orsi A.H., Johnson G.C. & Bullister J.L. 1999. Circulation, mixing, and production of Antarctic Bottom Water. *Progress in Oceanography 43*, 55–109.

Orsi A.H. & Wiederwohl C.L. 2009. A recount of Ross Sea waters. *Deep-Sea Research Part II 56*, 778–795.

Parish T.R. & Bromwich D.A. 1989. Instrumented aircraft observations of the katabatic wind regime near Terra Nova Bay. *Monthly Weather Review 117*, 1570–1585.

Pierrot D., Lewis E. & Wallace D.W.R. 2006. *MS Excel Program developed for CO_2 system calculations, ORNL/CDIAC-105*. Oak Ridge, TN: Carbon Dioxide Information Analysis Center, Oak Ridge National Laboratory, US Department of Energy.

Poisson A., Metzl N., Brunet C., Schauer B., Brès B., Ruiz-Pino D. & Louanchi F. 1993. Variability of sources and sinks of CO_2 in the western Indian and Southern oceans during the year 1991. *Journal of Geophysical Research—Oceans 98*, 22759–22778.

Reddy T.E., Arrigo K.R. & Holland D.M. 2007. The role of thermal and mechanical processes in the formation of the Ross Sea summer polynya. *Journal of Geophysical Research—Oceans 112*, C07027, doi: 10.1029/2006JC003874.

Redfield A.C., Ketchum B.H. & Richards F.A. 1963. The influence of organisms on the composition of sea water. In M.N. Hill (ed.): *The sea.* Vol. 2. Pp. 26–77. New York: Interscience.

Rivaro P., Bergamasco A., Budillon G., Frache R., Hohmann R., Massolo S. & Spezie G. 2004. Chlorofluorocarbon distribution in the Ross Sea water masses. *Chemistry and Ecology 20, Supplement 1*, S29–S41.

Rivaro P., Ianni C., Massolo S., Abelmoschi M.L., De Vittor C. & Frache R. 2011. Distribution of dissolved labile and particulate iron and copper in Terra Nova Bay polynya (Ross Sea, Antarctica) surface waters in relation to nutrients and phytoplankton growth. *Continental Shelf Research 31*, 879–889.

Rivaro P., Massolo S., Bergamasco A., Castagno P. & Budillon G. 2010. Chemical evidence of the changes of the Antarctic Bottom Water ventilation in the western Ross Sea between 1997 and 2003. *Deep-Sea Research Part I 57*, 639–652.

Rivaro P., Messa R., Massolo S. & Frache R. 2010. Distributions of carbonate properties along the water column in the Mediterranean Sea: spatial and temporal variations. *Marine Chemistry 121*, 236–245.

Roy R.N., Roy L.N., Vogel K.M., Moore C.P., Pearson T., Good E.C., Millero F.J. & Campbell D.M. 1993. The dissociation constants of carbonic acid in seawater at salinities 5 to 45 and temperatures 0 to 45°C. *Marine Chemistry 44*, 249–267.

Rubino A., Budillon G., Pierini S. & Spezie G. 2003. A model for the spreading and sinking of the Deep Ice Shelf Water in the Ross Sea. *Antarctic Science 15*, 25–30.

Sabine C.L., Feely R.A., Gruber N., Key R.M., Lee K., Bullister J.L., Wanninkhof R., Wong C.S., Wallace D.W.R., Tilbrook B., Millero F.J., Peng T., Kozyr A., Ono T. & Rios A.F. 2004. The oceanic sink for anthropogenic CO_2. *Science 305*, 367–371.

Sandrini S., Aït-Ameur N., Rivaro P., Massolo S., Touratier F., Tositti L. & Goyet C. 2007. Anthropogenic carbon distribution in the Ross Sea (Antarctica). *Antarctic Science 19*, 395–407.

Smethie W.M. Jr. & Jacobs S.S. 2005. Circulation and melting under the Ross Ice Shelf: estimates from evolving CFC, salinity and temperature fields in the Ross Sea. *Deep-Sea Research Part I 52*, 959–978.

Smith W.O. Jr., Dinniman M.S., Klinck J.M. & Hofmann E. 2003. Biogeochemical climatologies in the Ross Sea, Antarctica, seasonal patterns of nutrients and biomass. *Deep-Sea Research Part II 50*, 3083–3101.

Smith W.O. Jr. & Nelson D.M. 1985. Phytoplankton bloom produced by a receding ice edge in the Ross Sea: spatial coherence with the density field. *Science 227*, 163–166.

Smith W.O. Jr., Nelson D.M., DiTullio G.R. & Leventer A.R. 1996. Temporal and spatial patterns in the Ross Sea: phytoplankton biomass, elemental composition, productivity

Citation: *Polar Research* 2014, *33*, 20403, http://dx.doi.org/10.3402/polar.v33.20403

and growth rates. *Journal of Geophysical Research—Oceans 101*, 18455–18466.

Sweeney C. 2003. The annual cycle of surface water CO_2 and O_2 in the Ross Sea: a model for gas exchange on the continental shelves of Antarctica. In G. Di Tullio & R.B. Dunbar (eds.): *Biogeochemistry of the Ross Sea*. Pp. 295–312. Washington, DC: American Geophysical Union.

Sweeney C., Hansell D.A., Carlson C.A., Codispoti L.A., Gordon L.I., Marra J., Millero F.J., Smith W.O. & Takahashi T. 2000. Biogeochemical regimes, net community production and carbon export in the Ross Sea, Antarctica. *Deep-Sea Research Part II 47*, 3369–3394.

Tagliabue A. & Arrigo K.R. 2006. Processes governing the supply of iron to phytoplankton in stratified seas. *Journal of Geophysical Research—Oceans 111*, C06019, doi: 10.1029/2005JC003363.

Takahashi T., Sutherland S.C., Sweeney C., Poisson A., Metzl N., Tilbrook B., Bates N., Wanninkhof R., Feely R.A., Sabine C., Olafsson J. & Nojiri Y. 2002. Global sea–air CO_2 flux based on climatological surface ocean pCO_2, and seasonal biological and temperature effects. *Deep-Sea Research Part II 49*, 1601–1622.

Tortell P.D., Guéguen C., Long M.C., Payne C.D., Leeand P. & Di Tullio G.R. 2011. Spatial variability and temporal dynamics of surface water pCO_2, ΔO_2/Ar and dimethylsulfide in the Ross Sea, Antarctica. *Deep-Sea Research Part I 58*, 241–259.

Tremblay J.E. & Smith W.O. Jr. 2007. Primary production and nutrient dynamics in polynyas. In W.O. Smith & D.G. Barber (eds.): *Polynyas: windows to the world*. Pp. 239–269. Amsterdam: Elsevier.

UNESCO (United Nations Educational, Scientific and Cultural Organization) 1988. The acquisition, calibration, and analysis of CTD data. *A report of SCOR Working Group 51. UNESCO Technical Papers in Marine Science 54*. Paris: United Nations Educational, Scientific and Cultural Organization.

Wanninkhof R. 1992. Relationship between wind speed and gas exchange over the ocean. *Journal of Geophysical Research—Oceans 97*, 7373–7382.

Wanninkhof R. & McGillis W.R. 1999. A cubic relationship between sea–air CO_2 exchange and wind speed. *Geophysical Research Letters 26*, 1889–1892.

Weiss R.F. 1974. Carbon dioxide in water and seawater: the solubility of a non-ideal gas. *Marine Chemistry 2*, 203–215.

Weiss R.F. & Price B.A. 1980. Nitrous oxide solubility in water and seawater. *Marine Chemistry 8*, 347–359.

Whitworth T., III, Orsi A.H., Kim S.J. & Nowlin W.D. Jr. 1998. Water masses and mixing near the Antarctic slope front. In S.S. Jacobs & R.F. Weiss (eds.): *Ocean, ice, and atmosphere: interactions at the Antarctic continental margin*. Pp. 1–27. Washington, DC: American Geophysical Union.